

5-2-2017

A Novel Agonist of the TRIF Pathway Induces a Cellular State Refractory to Replication of Zika, Chikungunya, and Dengue Viruses.

Kara M Pryke

Jinu Abraham

Tina M Sali

Bryan J Gall

Iris Archer

See next page for additional authors

Follow this and additional works at: <https://digitalcommons.psjhealth.org/publications>

 Part of the [Infectious Disease Commons](#)

Recommended Citation

Pryke, Kara M; Abraham, Jinu; Sali, Tina M; Gall, Bryan J; Archer, Iris; Liu, Andrew; Bambina, Shelly; Baird, Jason R; Gough, Michael J.; Chakhtoura, Marita; Haddad, Elias K; Kirby, Ilsa T; Nilsen, Aaron; Streblow, Daniel N; Hirsch, Alec J; Smith, Jessica L; and DeFilippis, Victor R, "A Novel Agonist of the TRIF Pathway Induces a Cellular State Refractory to Replication of Zika, Chikungunya, and Dengue Viruses." (2017). *Articles, Abstracts, and Reports*. 1555.
<https://digitalcommons.psjhealth.org/publications/1555>

This Article is brought to you for free and open access by Providence St. Joseph Health Digital Commons. It has been accepted for inclusion in Articles, Abstracts, and Reports by an authorized administrator of Providence St. Joseph Health Digital Commons. For more information, please contact digitalcommons@providence.org.

Authors

Kara M Pryke, Jinu Abraham, Tina M Sali, Bryan J Gall, Iris Archer, Andrew Liu, Shelly Bambina, Jason R Baird, Michael J. Gough, Marita Chakhtoura, Elias K Haddad, Ilsa T Kirby, Aaron Nilsen, Daniel N Streblow, Alec J Hirsch, Jessica L Smith, and Victor R DeFilippis

A Novel Agonist of the TRIF Pathway Induces a Cellular State Refractory to Replication of Zika, Chikungunya, and Dengue Viruses

[Kara M. Pryke](#),^a [Jinu Abraham](#),^a [Tina M. Sali](#),^a [Bryan J. Gall](#),^a [Iris Archer](#),^a [Andrew Liu](#),^a [Shelly Bambina](#),^c [Jason Baird](#),^c [Michael Gough](#),^c [Marita Chakhtoura](#),^d [Elias K. Haddad](#),^d [Ilsa T. Kirby](#),^b [Aaron Nilsen](#),^b [Daniel N. Streblow](#),^a [Alec J. Hirsch](#),^a [Jessica L. Smith](#),^a and [Victor R. DeFilippis](#)^{✉a}

Terence S. Dermody, Editor

Terence S. Dermody, University of Pittsburgh School of Medicine;

^aVaccine and Gene Therapy Institute, Oregon Health and Science University, Portland, Oregon, USA

^bVeterans Affairs Medical Center, Portland, Oregon, USA

^cEarle A. Chiles Research Institute, Robert W. Franz Cancer Center, Providence Portland Medical Center, Portland, Oregon, USA

^dDivision of Infectious Diseases and HIV Medicine, Drexel College of Medicine, Philadelphia, Pennsylvania, USA

[✉]Corresponding author.

Address correspondence to Victor R. DeFilippis, defilipp@ohsu.edu.

K.M.P. and J.A. contributed equally to the completion of this work.

Received 2017 Mar 20; Accepted 2017 Apr 11.

[Copyright](#) © 2017 Pryke et al.

This is an open-access article distributed under the terms of the [Creative Commons Attribution 4.0 International license](https://creativecommons.org/licenses/by/4.0/).

ABSTRACT

The ongoing concurrent outbreaks of Zika, Chikungunya, and dengue viruses in Latin America and the Caribbean highlight the need for development of broad-spectrum antiviral treatments. The type I interferon (IFN) system has evolved in vertebrates to generate tissue responses that actively block replication of multiple known and potentially zoonotic viruses. As such, its control and activation through pharmacological agents may represent a novel therapeutic strategy for simultaneously impairing growth of multiple virus types and rendering host populations resistant to virus spread. In light of this strategy's potential, we undertook a screen to identify novel interferon-activating small molecules. Here, we describe 1-(2-fluorophenyl)-2-(5-isopropyl-1,3,4-thiadiazol-2-yl)-1,2-dihydrochromeno[2,3-*c*]pyrrole-3,9-dione, which we termed AV-C. Treatment of human cells with AV-C activates innate and interferon-associated responses that strongly inhibit replication of Zika, Chikungunya, and dengue viruses. By utilizing genome editing, we investigated the host proteins essential to AV-C-induced cellular states. This showed that the compound requires a TRIF-dependent signaling cascade that culminates in IFN regulatory factor 3 (IRF3)-dependent expression and secretion of type I interferon to elicit antiviral responses. The other canonical IRF3-terminal adaptor proteins STING and IPS-1/MAVS were dispensable for AV-C-induced phenotypes. However, our work revealed an important inhibitory role for IPS-1/MAVS, but not TRIF, in flavivirus replication, implying that TRIF-directed viral evasion may not occur. Additionally, we show that in response to AV-C, primary human peripheral blood mononuclear cells secrete proinflammatory cytokines that are linked with establishment of adaptive immunity to viral pathogens. Ultimately, synthetic innate immune activators such as AV-C may serve multiple therapeutic purposes, including direct antimicrobial responses and facilitation of pathogen-directed adaptive immunity.

KEYWORDS: antiviral agents, emerging virus, innate immunity, interferons

IMPORTANCE

The type I interferon system is part of the innate immune response that has evolved in vertebrates as a first line of broad-spectrum immunological defense against an unknowable diversity of microbial, especially viral, pathogens. Here, we characterize a novel small molecule that artificially activates this response and in so doing generates a cellular state antagonistic to growth of currently emerging viruses: Zika virus, Chikungunya virus, and dengue virus. We also show that this molecule is capable of eliciting cellular responses that are predictive of establishment of adaptive immunity. As such, this agent may represent a powerful and multipronged therapeutic tool to combat emerging and other viral diseases.

INTRODUCTION

The spontaneity and clinical impact of emerging mosquito-transmitted viral pathogens are illustrated exceptionally well by the recent appearance of Chikungunya virus (CHIKV) and Zika virus (ZIKV) in Latin America and the Caribbean (1). The preexisting transmission of dengue virus (DENV) across this geographic region (2) has resulted in cocirculation of three substantially pathogenic arboviruses that exhibit similar acute symptomatology for which long-term sequelae are also known (3, 4). This cocirculation not only renders differential diagnoses more complicated (5) but also may lead to enhanced but unknown disease manifestations during viral coinfection (6). Unfortunately, no FDA-approved antiviral treatments are currently available for any of these agents, and vaccines are only in use for DENV.

CHIKV is an *Alphavirus* that first emerged in the Americas in late 2013 (7) and has infected over a million people in the region since then (8). Acute infection is associated with febrile illness and debilitating joint pains but may also induce central nervous system disease, especially in neonates. While immunity is believed to be lifelong, severe joint pain may persist for months to years (9). ZIKV is a member of the *Flaviviridae* and dramatically emerged in the Americas in 2015 and 2016. As of this writing, 50 countries in the Americas have reported autochthonous transmission of the virus (<http://www.cdc.gov/zika/geo/active-countries.html>). The World Health Organization (WHO) has estimated that 3 to 4 million individuals will be infected with ZIKV in the coming year (10). It is estimated that 80% of acute ZIKV infections are asymptomatic, with the remaining 20% clinically resembling infection by CHIKV and DENV, including fever, rash, headache, and arthralgia, although ZIKV appears to be distinctly associated with conjunctivitis (11). Neurological complications, including Guillain-Barré syndrome, have also been reported following ZIKV infection (12). Most importantly, however, ZIKV infection during pregnancy is associated with severe teratogenic effects, including microcephaly (13). As such, the need for prophylactic and therapeutic strategies to combat these pathogens is extremely high.

The type I interferon (IFN) system represents an antiviral response that is shared by all vertebrates and has thus been evolutionarily shaped by exposure through millennia to an unknowable diversity of pathogens (14). The outcome is a cell-based protective response that exhibits efficacy against a phylogenetically broad range of viruses that are both ubiquitous and potentially harmful. Type I IFNs (multiple IFN- α subtypes and IFN- β) are cytokines that bind the IFN- α receptor (IFNAR) present on nearly all cells and induce signaling via Janus kinases (JAKs) to the protein signal transducer and activator of transcription 1 (STAT1) and STAT2. These proteins activate synthesis of hundreds of IFN-stimulated genes (ISGs), many of which confer direct antiviral effects by generating a cellular state antagonistic to virus growth, while others facilitate and coordinate adaptive immune responses (15). IFNs themselves are transcribed and secreted in response to cellular detection of pathogen-associated molecular patterns (PAMPs). This process is triggered by pattern recognition receptors (PRRs) that, in response to PAMP engagement, initiate signaling cascades that culminate in the activation of transcription factors such as IFN regulatory factor 3 (IRF3) and nuclear factor κ B (NF- κ B) (reviewed in reference 16). These, in turn, transcribe IFNs as well as other proinflammatory cytokines and antiviral effectors. Three principal PRR-driven, IRF3-terminal pathways defined by their unique adaptor proteins are known and include IFN promoter stimulator 1 (IPS-1, also known as MAVS, VISA, or CARDIF), which integrates signaling from the PRRs of cytoplasmic double-stranded RNA (dsRNA) RIG-I and MDA5 (17,–20), the stimulator of IFN genes protein (STING; also known as MITA, ERIS, MPYS, or TMEM173), which is both a PRR for cyclic dinucleotides and an adaptor for PRRs of cytoplasmic dsDNA (21,–25), and Toll/interleukin-1 (IL-1) receptor domain-containing adapter activating IFN (TRIF, also known as TICAM), which transmits signaling from Toll-like receptor 3 (TLR3) and TLR4 (26, 27). Together, these pathways are capable of stimulating the IFN response following exposure to a wide array of molecular indicators of microbial infection.

Given the phenotypic potency and target breadth of the type I IFN system, it has been utilized as a host-directed method to block virus infection. In fact, treatment with various forms of IFN itself has demonstrated clinical success against hepatitis B and C viruses (28,–30). However, use of systemic IFNs is associated with substantial undesirable effects. For instance, extraordinarily high doses of IFN, such as those administered during conventional therapy, are associated with multiple potentially severe side effects, most notably neurotoxicity and neuropsychiatric complications (31, 32) that contribute to voluntary cessation of treatment. Additionally, clinical-grade IFN is costly to produce and requires repeated delivery due to a short *in vivo* half-life, and these factors contribute to a high overall expense. Alternatively, pharmacological induction of IFN-dependent responses has been pursued as a strategy to combat viral infection (33). Experimental induction of IFN synthesis via administration of PAMPs or small molecules has also proven efficacious against multiple virus types *in vitro* and *in vivo* (34,–40). This includes recent work from our group in which we described a novel small-molecule agonist of the human STING pathway that elicits antiviral effects against alphaviruses, including CHIKV (41). Furthermore, targeted activation of innate cytokine responses can also be harnessed for other therapeutic outcomes, such as vaccine adjuvanticity (42) and antitumor responses (43), thus providing multiple potential clinical uses. Importantly, given that the effects of IFN are broad with respect to known viral pathogens, it is virtually certain that numerous unknown, potentially emerging, and zoonotic virus types are similarly susceptible to IFN-induced cellular states. As such, pharmacological IFN activation may represent a cost-effective and impactful antiviral strategy applicable for populations prone to virus emergence events. Moreover, the ability to simultaneously impair growth of multiple virus types by using a single therapy would be attractive in areas where transmission of multiple viruses is ongoing, such as current-day Latin America and the Caribbean. In light of this, we describe here a novel small molecule capable of rendering human cells inhibitory to growth of ZIKV, CHIKV, and DENV and of eliciting proinflammatory responses from human immune cells. By using deeper molecular analysis, we show that the cellular target of this compound is the IRF3-terminal TRIF pathway.

RESULTS

Compound AV-C induces type I IFN-dependent transcription in human fibroblasts. To identify novel small molecules capable of activating innate immune responses in human cells, we employed foreskin fibroblasts stably transfected with constitutively expressed human telomerase reverse transcriptase for prevention of senescence (44). The luciferase (LUC) open reading frame from *Phytionis pyralis* downstream of a promoter element that is activated by type I IFN-mediated cell signaling was stably introduced by lentiviral transduction (THF-ISRE), as described elsewhere (45). Using these cells in a high-throughput screening platform, we examined approximately 51,000 chemically diverse compounds in duplicate for their ability to significantly stimulate LUC expression (41). One stimulatory molecule was 1-(2-fluorophenyl)-2-(5-isopropyl-1,3,4-thiadiazol-2-yl)-1,2-dihydrochromeno[2,3-*c*]pyrrole-3,9-dione, which we termed AV-C (Fig. 1A; see also Fig. S1 in the supplemental material). We next performed a follow-up experiment to both validate the screening results and examine whether dose-dependent LUC synthesis occurred. As shown in Fig. 1B, exposure of THF-ISRE cells to media containing AV-C resulted in concentration-associated expression of IFN-dependent LUC. These results suggest that the molecule triggers an innate cellular response that stimulates IFN-dependent signaling in human fibroblasts.

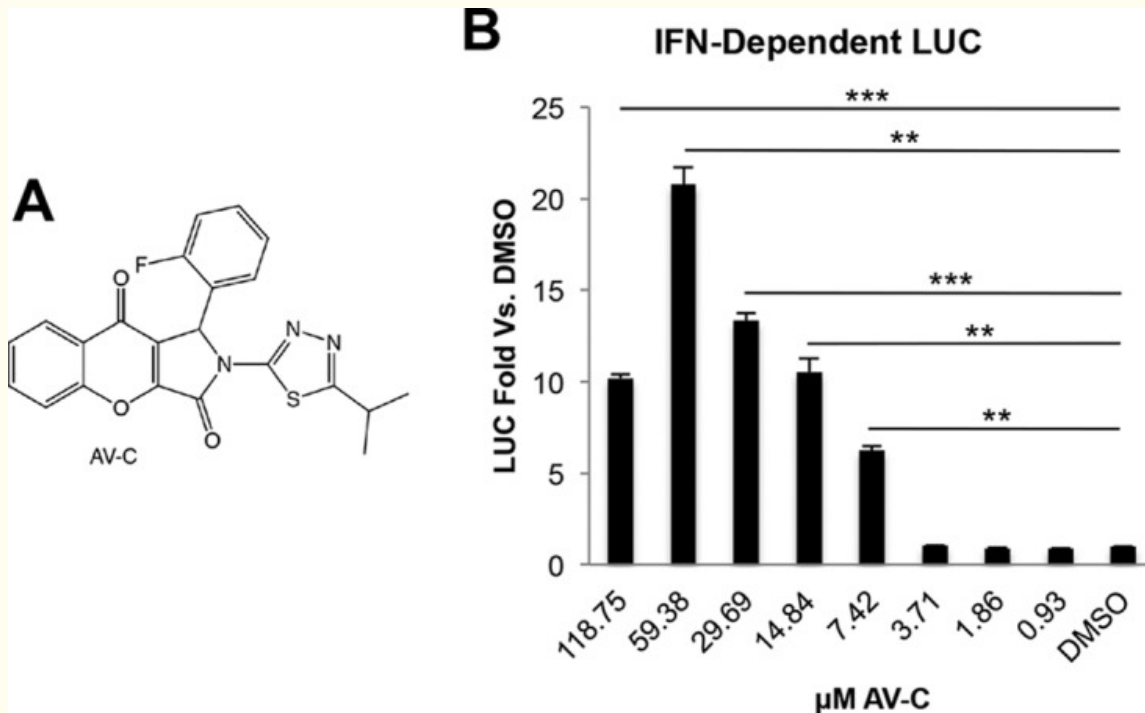


FIG 1

Activation of type I interferon-associated transcription after exposure to AV-C. (A) Chemical structure of 1-(2-fluorophenyl)-2-(5-isopropyl-1,3,4-thiadiazol-2-yl)-1,2-dihydrochromeno[2,3-c]pyrrole-3,9-dione (AV-C). (B) Reporter assay results, showing induction of ISRE-dependent LUC expression in THF-ISRE cells at 8 h posttreatment at the indicated concentrations. Values displayed are average fold changes \pm standard deviations, based on three replicates in comparison to results in DMSO-treated cells. Unpaired-sample Student's *t* test comparisons were made between AV-C- and DMSO-treated cells. **, $P \leq 0.01$; ***, $P \leq 0.001$.

FIG S1

High-throughput identification of AV-C. Luciferase (LUC) expression of the top activating molecules as described in the text from a high-throughput screen of 51,632 compounds. Presented values represent the average \pm standard deviation of results from duplicate assays. The black bar and arrow indicate the LUC signal generated by AV-C. Download [FIG S1](#), [PDF file](#), [0.1 MB](#).

[Copyright](#) © 2017 Pryke et al.

This content is distributed under the terms of the [Creative Commons Attribution 4.0 International license](#).

AV-C activates transcription and translation of antiviral effector genes. Since AV-C efficiently activated expression of a heterologous IFN-dependent reporter, we next examined the degree to which the molecule could also induce transcription of endogenous genes, in particular those that are known to be downstream of IFN pathways. For this, we utilized genomic hybridization-based microarrays. THF cells were treated in duplicate with 1% dimethyl sulfoxide (DMSO; mock treatment), 25 μ M AV-C, or 1,000 U/ml IFN- β for 8 h. Total RNA was harvested, and probes complementary to mRNA were synthesized and hybridized to Affymetrix Primeview microarrays as described in Materials and Methods. Probe sets exhibiting signals from AV-C or IFN- β treatments that were significantly above or below those from mock-treated cells were then statistically retrieved using analysis of variance (ANOVA) as implemented within the Affymetrix transcriptome analysis console. [Figure 2A](#) displays in heat map format all individual probe sets from each treatment that were found to exhibit differential signals relative to mock-treated cells following exposure to either AV-C or IFN- β . The Venn diagrams in [Fig. 2B](#)

illustrate that 113 annotated coding regions were co-upregulated and 28 were co-downregulated in response to AV-C and IFN- β treatments. Moreover, 1,205 and 126 genes were uniquely upregulated in response to IFN- β and AV-C treatments, respectively, and 1,365 and 50 genes were uniquely downregulated in response to IFN- β and AV-C treatments, respectively. Individual fold changes for all regulated genes are included in [Table S1](#). Interestingly, among the mRNAs coinduced between AV-C and IFN- β treatments were many known to encode proteins that confer directly antiviral phenotypes, including Mx1 (46), IFIT1 (47), RSAD2/Viperin (48), and OAS1 (49). Moreover, microarray results indicated that AV-C induced the transcription of IFN- β itself which, if translated and secreted, would presumably lead to ISG expression via autocrine/paracrine signaling. Intriguingly, other immune-associated mRNAs that are involved in inflammatory and adaptive immune responses were exclusively induced by treatment with AV-C but not IFN- β , including PTGS2/COX-2 (50), CCL5 (51), CXCL8/IL-8 (52), and IL-6 (53). We next examined whether translation of coregulated antiviral proteins was also detectable in response to treatment with AV-C, a requirement for establishment of an antiviral cellular state. As shown in [Fig. 2C](#), both IFN- β and AV-C triggered the synthesis of antiviral proteins Mx1 and IFIT1, suggesting that AV-C is likely to alter the innate phenotypic condition of cells exposed to it. Whether the transcriptional induction program generated by exposure to AV-C is sufficient to block virus replication was next investigated in light of these findings.

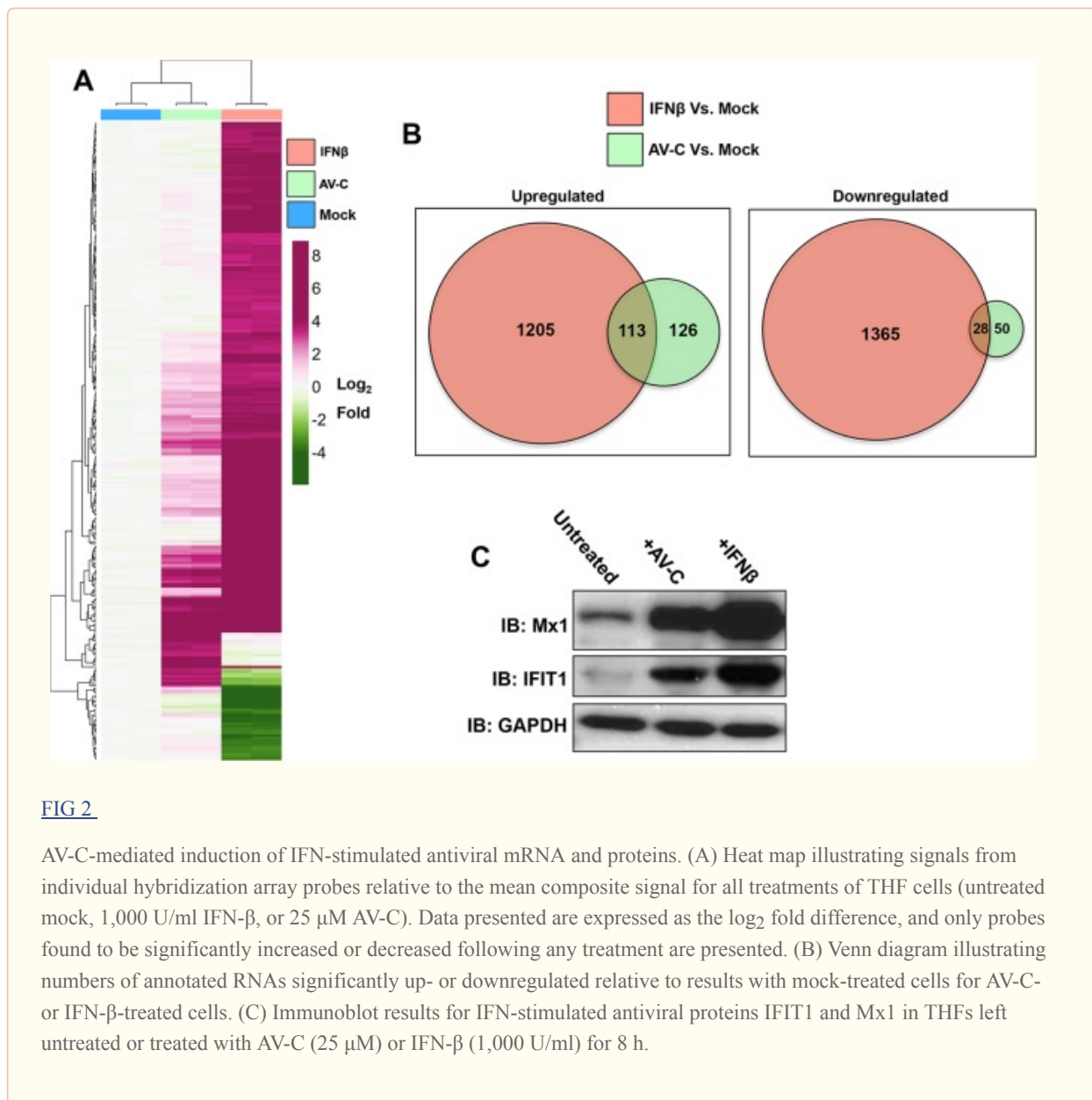


TABLE S1

Absolute fold changes relative to overall mean signals in mock-treated cells of individual Affymetrix probe sets found to be differentially regulated following treatment with either AV-C or IFN- β . Download [TABLE S1, XLS file, 0.3 MB](#).

Copyright © 2017 Pryke et al.

This content is distributed under the terms of the [Creative Commons Attribution 4.0 International license](#).

AV-C elicits a cellular state that inhibits replication of ZIKV, CHIKV, and DENV. Based on our observations that AV-C activates transcription and translation of known antiviral effector genes as well as IFN- β itself, we hypothesized that cells preexposed to the compound would be refractory to virus growth. To address this, we examined replication of CHIKV, ZIKV, and DENV on AV-C-treated fibroblasts; these three geographically cooccurring mosquito-transmitted viruses are of recent and extraordinary clinical importance (1, 54). Human fibroblasts represent a permissive and crucial cell type for CHIKV and ZIKV and thus constitute a biologically relevant *in vitro* model for these pathogens (55, 56). THF cells were first pretreated with AV-C over a range of molarities for 6 h. Cells were then infected with CHIKV, ZIKV, or DENV in the presence of AV-C for the indicated durations. As shown in Fig. 3, treatment with AV-C diminished replication of CHIKV and ZIKV by multiple logs, displaying 90% inhibitory concentrations (IC₉₀) of 5.815 μ M (ZIKV) and 3.538 μ M (CHIKV), which are well below dosages observed to induce detectable cytotoxicity (Fig. S2). DENV, in contrast, did not grow to comparable peak titers on these cells, an observation we hypothesize is due to the virus' relative inability to counteract existing antiviral innate signaling in these cells (see below). Nevertheless, DENV still showed sensitivity to AV-C, with an IC₉₀ of 9.939 μ M. Based on these results, we concluded that, despite not inducing a fully overlapping subset of IFN-stimulated genes (Fig. 2), AV-C treatment nevertheless generates a cellular state that is antagonistic to replication of DENV, CHIKV, and ZIKV. Among these viruses, CHIKV clearly demonstrated the highest degree of susceptibility to the AV-C-induced cellular state, with an approximately 4-log peak reduction in virus titer. ZIKV was also highly sensitive, however, exhibiting an approximately 2.5-log titer reduction.

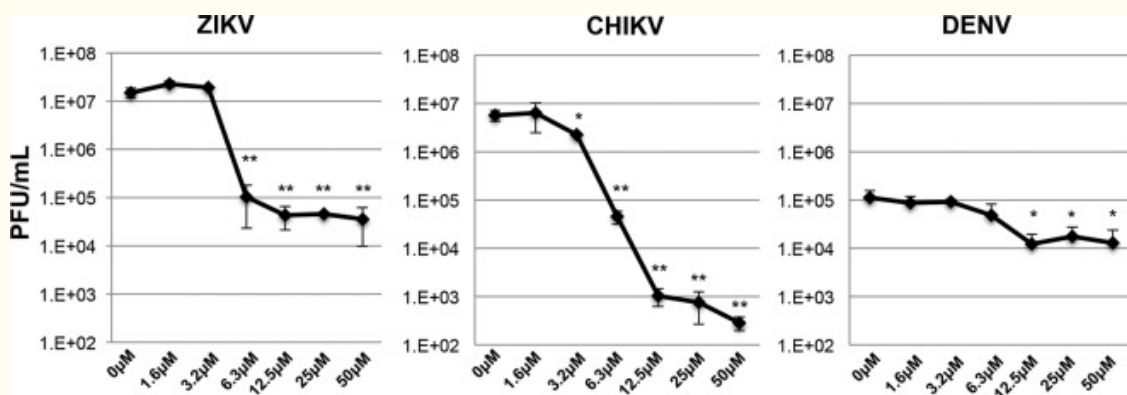


FIG 3

AV-C elicits a cellular state refractory to virus replication. Average results (PFU per milliliter, \pm the standard deviation) of ZIKV, CHIKV, and DENV grown on THF cells in triplicate in the presence of the indicated AV-C concentrations (the DMSO concentration was normalized to 1%) added 6 h preinfection. Unpaired-sample Student's *t* test comparisons were made between AV-C- and DMSO-treated cells. **, $P \leq 0.01$; ***, $P \leq 0.001$.

FIG S2

ATP-dependent luminescence of THF following 24-h or 48-h exposure to the indicated concentrations of AV-C (with the DMSO concentration normalized to 3%). Values displayed are raw luminescence values averaged from quadruplicate measurements (\pm standard deviations) following 24-h or 48-h exposure to the indicated concentration of AV-C. Download [FIG S2](#), [PDF file](#), [0.1 MB](#).

[Copyright](#) © 2017 Pryke et al.

This content is distributed under the terms of the [Creative Commons Attribution 4.0 International license](#).

Alphaviruses and flaviviruses possess evolutionarily analogous yet biologically potent phenotypes to counteract the antiviral effects of IFN stimulation (reviewed in references [57](#) and [58](#)). We therefore asked whether AV-C could inhibit virus growth when it was added to cells after infection, a circumstance that would potentially allow its use in therapeutic treatment. To address this, we exposed THF-ISRE cells to AV-C at different times relative to viral inoculation. As shown in [Fig. S3](#), AV-C lost its ability to block CHIKV growth when added 2 h postinfection, a finding consistent with the appearance of alphavirus innate evasion proteins ([59](#)). Since ZIKV exhibited higher overall sensitivity to AV-C than did DENV ([Fig. 3](#)), likely an effect of cell permissivity, we examined the effect of AV-C added postinfection on the growth of a representative flavivirus. In this case, inhibition by AV-C was evident as late as 16 h postinfection, indicating either that the compound exhibits antiviral effects that are virus type specific or that the ZIKV IFN evasion phenotypes are expressed much later in infection than those against CHIKV.

FIG S3

Effect of AV-C time of addition on virus replication. Average results (in PFU per milliliter \pm the standard deviation) are shown for ZIKV and CHIKV grown on THF cells in triplicate in the presence of 12.5 μ M AV-C (the DMSO concentration was normalized to 1%) added to cells at the indicated times pre- or postinfection. Medium was harvested at 48 h (CHIKV) or 72 h (DENV and ZIKV) postinfection, and titers were determined based on serial dilution PFU (CHIKV) or FFU (ZIKV and DENV) assay on Vero cells. Download [FIG S3](#), [PDF file](#), [0.1 MB](#).

[Copyright](#) © 2017 Pryke et al.

This content is distributed under the terms of the [Creative Commons Attribution 4.0 International license](#).

AV-C-induced gene expression requires IRF3 phosphorylation and canonical IRF3 kinase activity. AV-C stimulates expression of genes that are downstream of promoters activated by type I IFN as well as the IFN- β gene itself, and IRF3 is conventionally required for IFN synthesis. To begin to dissect the molecular basis of host cell responses to and targets of AV-C, we next investigated whether IRF3 is involved in innate activation by AV-C. First, we examined the phosphorylation status of IRF3 in response to AV-C exposure. As shown in [Fig. 4A](#), treatment of THF cells with stimuli activating the three key IRF3-terminal signaling pathways (discussed in more detail below) defined by the adaptor proteins IPS-1/MAVS (Sendai virus [SeV] [[20](#)]), STING (molecule G10 [[41](#)]), and TRIF (lipopolysaccharide [LPS] [[60](#)]), all activated IRF3 phosphorylation at 4 h posttreatment. Similarly, AV-C at 25 μ M also led to IRF3 phosphorylation in these cells, as well as numerous additional human cell types, including HeLa cells, HEK-293 cells, SK-N-MC neuronal cells, THP-1 promonocytic cells, and microvascular endothelial cells ([Fig. S4](#)). We next investigated whether IRF3 is functionally essential to AV-C-induced gene transcription. For this, we employed previously described THF-ISRE cells from which IRF3 was deleted via CRISPR/Cas9 technology (THF-ISRE- Δ IRF3) ([41](#)). As shown in [Fig. 4B](#), no detectable LUC expression was observed in these cells following treatment with multiple concentrations of AV-C or human cytomegalovirus particles rendered inactive by UV treatment (UV-HCMV), a STING-inducing stimulus ([61](#)). Importantly, IFN-dependent JAK/STAT signaling was operational in these cells, as demonstrated by LUC expression in response to IFN- β exposure. We next verified that AV-C-mediated induction of endogenous genes was similarly sensitive to the presence of IRF3. For this, semiquantitative reverse transcriptase (RT)-PCR (qPCR) was used to measure mRNA synthesis in THF-ISRE- Δ IRF3 cells following treatment with AV-C, SeV, or IFN- β relative to synthesis in cells treated with 1% DMSO. [Figure 4C](#) shows that only IFN- β stimulation led to mRNA induction of ISG15, IFIT1, and Mx2 and that no induction was seen with AV-C or the IPS-1/MAVS-activating

stimulus SeV. IRF3-dependent transcription requires phosphorylation-mediated activation of the protein by TANK binding kinase 1 (TBK1) or inducible I-kappa B kinase epsilon (IKK ϵ) (62). We therefore next examined whether AV-C activates canonical TBK1- or IKK ϵ -dependent IRF3 phosphorylation. THF-ISRE cells were treated with AV-C or UV-HCMV in the presence and absence of BX795, a small-molecule inhibitor of TBK1 and IKK ϵ kinase activities (63). As shown in Fig. 4D, treatment of THF-ISRE cells with UV-HCMV or AV-C in the presence, but not absence, of BX795 failed to stimulate LUC expression. Moreover, the immunoblotting results in Fig. 4E illustrate that exposure of cells to UV-HCMV or AV-C activated phosphorylation of IRF3, a process that does not occur in the presence of BX795. These results indicate that AV-C acts upstream of TBK1/IKK ϵ -mediated phosphorylation of IRF3 and subsequent IRF3-dependent gene transcription.

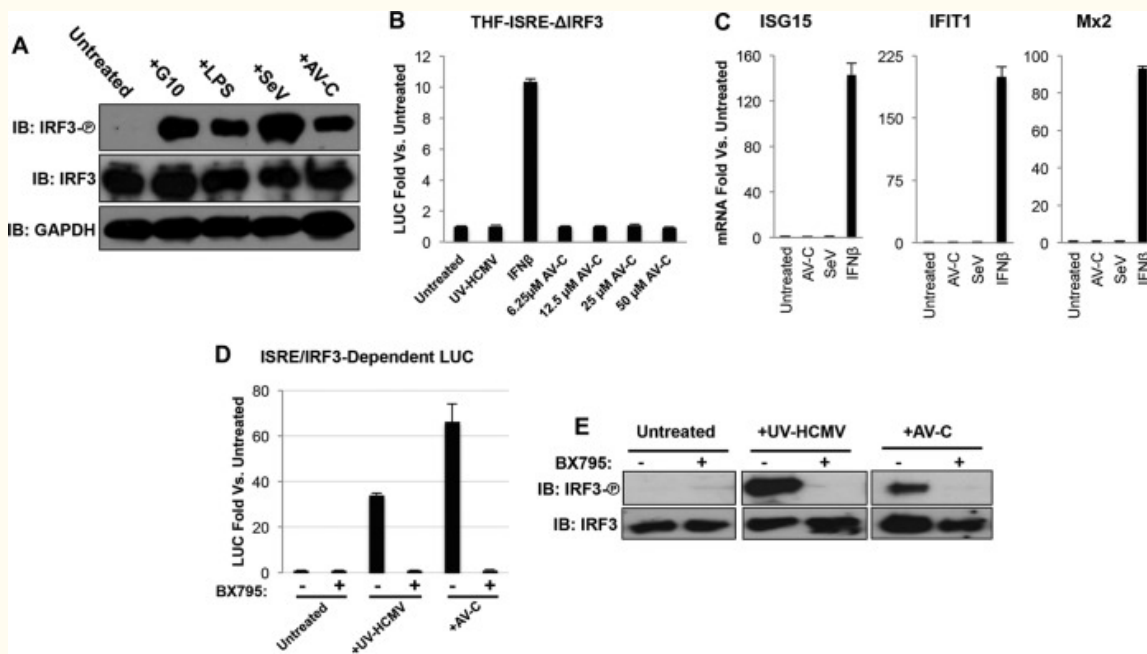


FIG 4

AV-C induces canonical IRF3 activation and IRF3- and IFN-dependent transcription. (A) Immunoblot results, showing S386 phosphorylation status of IRF3, total IRF3, and GAPDH from THF lysates following 4-h treatment with 1% DMSO (untreated), 100 μM G10, 1 ng/ml LPS, 160 HAU/ml SeV, or 25 μM AV-C. (B) Reporter assay results, showing induction of ISRE-dependent LUC expression in THF-ISRE cells lacking IRF3 following 8-h treatment with UV-inactivated HCMV (MOI, 3), 1,000 U/ml IFN-β, or AV-C at the indicated concentrations. Values displayed are average fold changes versus results in DMSO-treated cells of three replicates, ± the standard deviation (SD). (C) Transcription of ISG15, IFIT1, and Mx2 in cells treated for 8 h with 25 μM AV-C, SeV (160 HAU/ml), or 1,000 U/ml IFN-β. Values displayed are average fold changes versus results in DMSO-treated cells of two biological replicates, ± SD. (D) Reporter assay showing induction of LUC expression in THF-ISRE cells left untreated or exposed to UV-HCMV (MOI, 3) or 25 μM AV-C in the presence or absence of the TBK1/IKK ϵ inhibitor BX795 (10 nM). Values displayed are average fold changes versus results with DMSO-treated cells of three replicates, ± SD. (E) Immunoblot results, showing the S386 phosphorylation status of IRF3 as well as total IRF3 in THFs left untreated following 4-h exposure to UV-HCMV (MOI, 3) or 25 μM AV-C in the presence or absence of 10 nM BX795.

FIG S4

Immunoblots showing the phosphorylation status of IRF3 S386 and GAPDH (loading control) in HeLa, SK-N-M.C., HEK-293, THP-1, and TDMV-B cells either left untreated or following 4 h treatment with 25 μM AV-C. Download [FIG S4](#), [PDF file](#), 0.2 MB.

AV-C-mediated, IRF3-dependent innate activation occurs independently of adaptor proteins IPS-1/MAVS and STING but requires TRIF.

Conventional IRF3-terminal signaling pathways lead from PRRs via adaptor proteins to TBK1/IKK ϵ kinase and IRF3 activation. The adaptors include IPS-1/MAVS, which is required for signals initiated by the cytoplasmic dsRNA receptors RIG-I and MDA5 (17,–20), STING, which is both a cytoplasmic PRR of cyclic dinucleotides and also an adaptor for cytoplasmic receptors of dsDNA (23,–25, 64), and TRIF, which is essential for signaling initiated from TLR3 and TLR4, which sense dsRNA and LPS, respectively. Since all three are widely known to be essential components of defined signaling cascades that culminate in IRF3 phosphorylation, we hypothesized that at least one is required for innate stimulation by AV-C. To address this, we used previously described THF-ISRE cells lacking IPS-1/MAVS or STING (termed THF-ISRE- Δ IPS1 and THF-ISRE- Δ STING cells) (41) as well as newly constructed cells lacking TRIF (THF-ISRE- Δ TRIF cells).

As shown in Fig. 5, AV-C, but not the control stimulus SeV, was able to induce IFN-dependent LUC expression in THF-ISRE- Δ IPS1 cells. Furthermore, AV-C treatment also led to transcription of endogenous antiviral mRNAs for ISG15, IFIT1, Mx2, and viperin, whereas SeV treatment, as expected, did not result in transcription in the absence of IPS1/MAVS (Fig. 5B). Consistent with these results, AV-C was also able to activate IRF3 phosphorylation in cells lacking IPS-1/MAVS (Fig. 5C), as was the STING pathway agonist G10 (41), but not SeV. AV-C also induced expression of IFN-dependent LUC in cells lacking STING, in contrast to results with the control compound G10 (Fig. 5D). Additionally, AV-C, but not G10, was able to stimulate transcription of ISG15, IFIT1, Mx2, and viperin mRNAs (Fig. 5E), as well as IRF3 phosphorylation (Fig. 5F) in THF-ISRE- Δ STING cells.

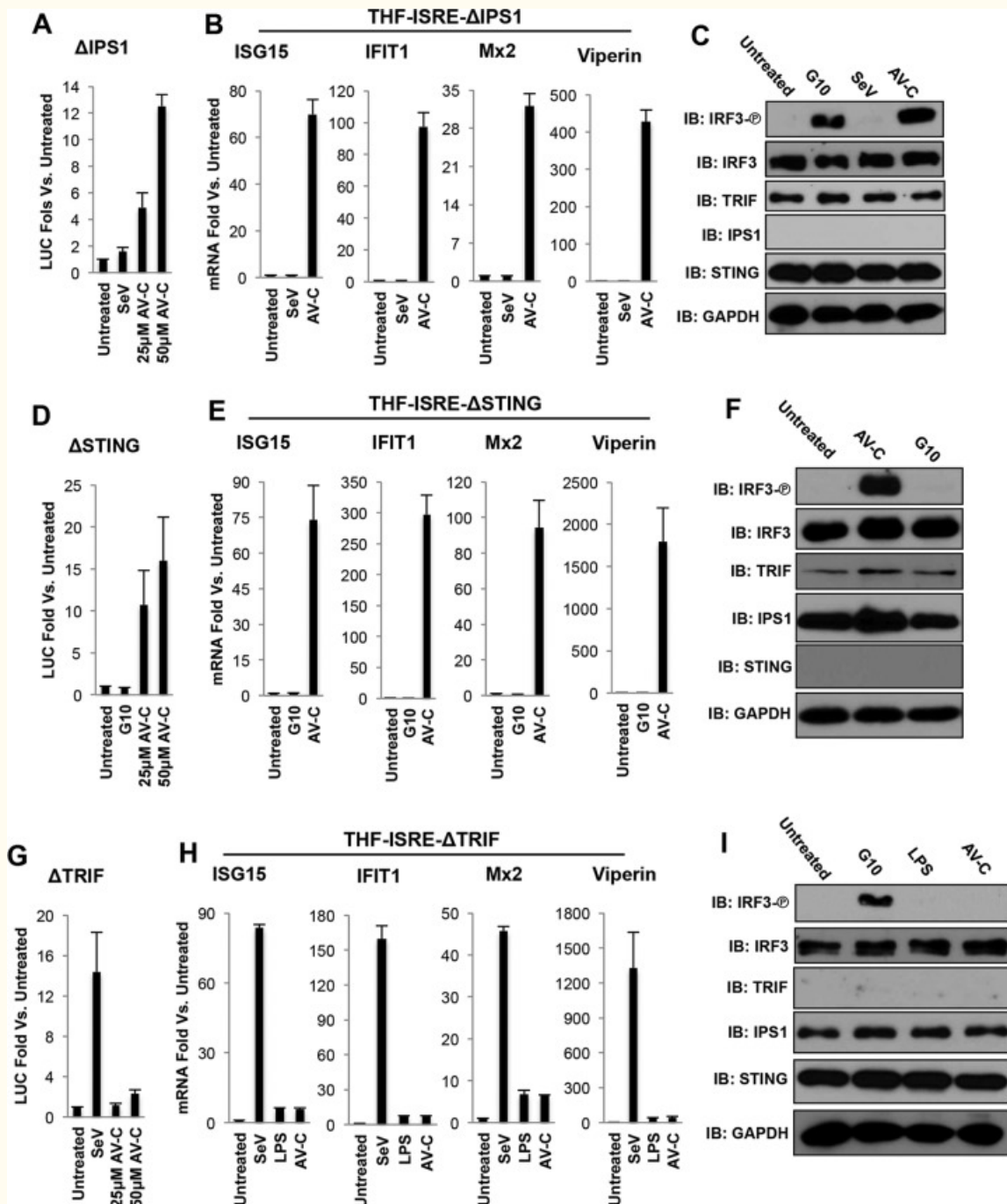


FIG 5

AV-C induces IRF3-mediated transcriptional activity in a manner independent of STING and IPS-1/MAVS but dependent on TRIF. (A) Reporter assay results, showing induction of ISRE-dependent LUC expression in THF-ISRE cells lacking IPS1/MAVS (THF-ISRE-ΔIPS1) following 8-h treatment with SeV (160 HAU/ml) or AV-C at the indicated concentrations. Values displayed are average fold changes compared to results with DMSO-treated cells of three replicates (\pm standard deviations [SD]). (B) Transcription of ISG15, IFIT1, viperin, and Mx2 in THF-ISRE-ΔIPS1 cells treated for 8 h with SeV (160 HAU/ml), or 50 μ M AV-C. Values displayed are average fold changes versus results in DMSO-treated cells of two biological replicates, \pm SD. (C) Immunoblot showing S386 phosphorylation status of IRF3 as well as total IRF3, TRIF, STING, IPS1/MAVS, and GAPDH in THF-ISRE-ΔIPS1 cells left untreated and following 4-h exposure to 100 μ M G10, SeV (160 HAU/ml), or 25 μ M AV-C. (D) Reporter assay results, showing induction of ISRE-dependent LUC expression in THF-ISRE cells lacking STING (THF-ISRE-ΔSTING) following 8-h treatment with 100 μ M G10 or AV-C at the indicated concentrations. Values displayed are average fold changes compared to results in DMSO-treated cells of three replicates, \pm SD. (E) Transcription of ISG15,

IFIT1, viperin, and Mx2 in THF-ISRE- Δ STING cells treated for 8 h with 100 μ M G10 or 25 μ M AV-C. Values displayed are average fold changes compared to results in DMSO-treated cells of two biological replicates, \pm SD. (F) Immunoblot results showing the S386 phosphorylation status of IRF3 as well as total IRF3, TRIF, STING, IPS1/MAVS, and GAPDH in THF-ISRE- Δ STING cells left untreated and following 4-h exposure to 100 μ M G10 or 25 μ M AV-C. (G) Reporter assay results, showing induction of ISRE-dependent LUC expression in THF-ISRE cells lacking TRIF (THF-ISRE- Δ TRIF) following 8-h treatment with 100 μ M G10 or AV-C at the indicated concentrations. Values displayed are average fold changes compared to results in DMSO-treated cells of three replicates, \pm SD. (H) Transcription of ISG15, IFIT1, viperin, and Mx2 in THF-ISRE- Δ TRIF cells treated for 8 h with 100 μ M G10 or 25 μ M AV-C. Values displayed are average fold changes versus results in DMSO-treated cells of two biological replicates, \pm SD. (I) Immunoblot results, showing S386 phosphorylation status of IRF3 as well as total IRF3, TRIF, STING, IPS1/MAVS, and GAPDH in THF-ISRE- Δ TRIF cells left untreated and following 4-h exposure to 100 μ M G10 or 25 μ M AV-C.

We next examined whether AV-C triggered innate induction in the absence of TRIF. As shown in [Fig. 5G](#), while the IPS-1/MAVS-activating stimulus SeV was able to trigger substantial LUC signal in THF-ISRE- Δ TRIF cells, treatment with AV-C at 25 μ M or 50 μ M did not. Similarly, strong synthesis of ISG15, IFIT1, viperin, and Mx2 mRNA was observed in these cells following treatment with SeV but not with AV-C or the TLR4/TRIF agonist LPS ([Fig. 5H](#)). Consistent with these results, phosphorylation of IRF3 was only detected in THF-ISRE- Δ TRIF cells following treatment with SeV but not AV-C or LPS ([Fig. 5I](#)). Based on these observations, we conclude that the IRF3-terminal innate response induced by AV-C occurs via a STING- and IPS1/MAVS-independent but TRIF-dependent signaling pathway.

AV-C-induced antiviral activity requires TRIF- and IFNAR-dependent signaling. Our results indicated that IRF3-mediated responses elicited by AV-C, including expression of antiviral effectors, occurs in a manner dependent on TRIF but not IPS-1/MAVS or STING. We therefore examined whether similar functional relationships are evident with respect to antiviral cellular states induced by the molecule. We therefore pretreated THF-ISRE, THF-ISRE- Δ IPS1, THF-ISRE- Δ STING, and THF-ISRE- Δ TRIF cells with AV-C at 12.5 μ M, which is over twice the IC₉₀ for ZIKV, over 3.5 times the IC₉₀ for CHIKV, and 1.25 times the IC₉₀ for DENV on wild-type cells ([Fig. 3](#)). We also used IFN- β as a positive control and DMSO as the negative control and infected treated cells with CHIKV, DENV, or ZIKV, as described above. As shown in [Fig. 6A](#), replication of the three virus types was strongly impaired in all four mutant cell lines pretreated with IFN- β , indicating that their JAK/STAT-dependent antiviral responses were appropriately intact. In addition, AV-C pretreatment of THF-ISRE, THF-ISRE- Δ IPS1, and THF-ISRE- Δ STING cells also significantly diminished virus replication relative to that with the negative-control treatment, in agreement with the innate activation states presented in [Fig. 5](#). Viral growth in AV-C-treated cells lacking TRIF, however, appeared statistically similar to that observed following mock treatment of these cells. This observation also agrees with the identified role for TRIF in IRF3-mediated activity and shows that this relationship extends to the molecule's elicitation of an antiviral state.

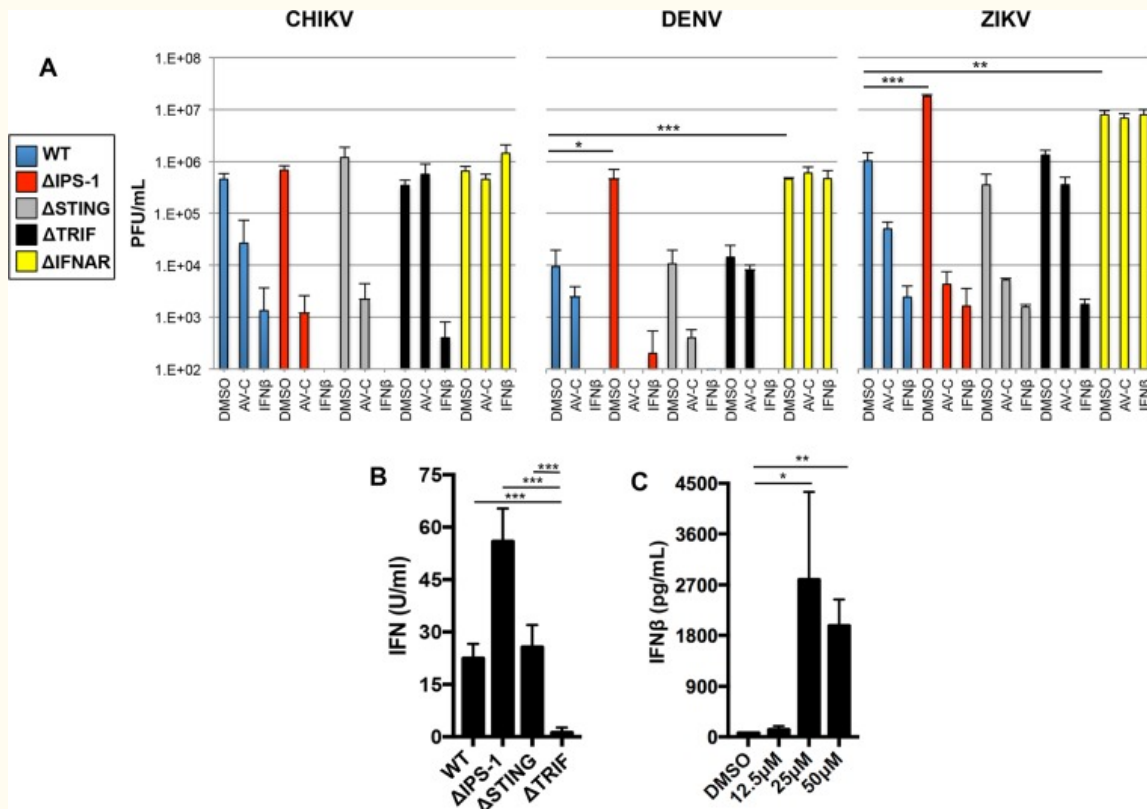


FIG 6

AV-C elicits an antiviral state in cells lacking the IPS-1/MAVS or STING pathways but not the TRIF or IFNAR pathways. (A) Average PFU per milliliter (\pm the standard deviation) for CHIKV, DENV, or ZIKV grown on wild-type (WT) THF-ISRE cells (blue) and THF-ISRE lacking IPS-1/MAVS (red), STING (gray), TRIF (black), or IFNAR (yellow) following 6 h pretreatment with 1% DMSO, 12.5 μ M AV-C, or 1,000 U/ml IFN- β (the DMSO concentration was normalized to 1%). Infections were performed in triplicate, and virus titers were determined by serial dilution plaque assay at 48 h postinfection (CHIKV) or by FFU assay at 72 h postinfection (ZIKV and DENV) as described in the text. (B) Average units per milliliter of type I IFN, as determined in a luciferase bioassay of levels secreted from the indicated cells following 8-h treatment with 12.5 μ M AV-C. (C) Average (in picograms per milliliter) \pm the standard deviation of secreted IFN- β , determined by ELISA from human PBMCs following 8-h treatment in triplicate with the indicated concentrations of AV-C. An unpaired Student's *t* test was used to determine statistical significance. *, $P < 0.05$; **, $P < 0.01$; ***, $P < 0.001$.

Given the profound susceptibility of CHIKV, DENV, and ZIKV to IFN-induced cellular states and the functional link between IRF3 activation and IFN synthesis, we decided to additionally ask whether AV-C-induced, TRIF-dependent antiviral activity also required IFN-dependent signaling. Moreover, while AV-C induces transcription of IFN- β (Fig. 2), it also stimulates expression of ISGs such as ISG15, IFIT1, and viperin, which confer antiviral activity but can also be induced by IRF3 alone, in the absence of IFN (65, 66). To address this, we used CRISPR/Cas9 to construct THF-ISRE cells lacking the type I IFN receptor IFNAR (THF-ISRE- Δ IFNAR cells). As shown in Fig. 6A, pretreatment of these cells with IFN- β had no effect on the growth of any of the three viruses relative to control pretreatment, phenotypically validating the IFNAR deletion. Interestingly, AV-C pretreatment also failed to elicit a block to virus replication in these cells (Fig. 6A), indicating that the AV-C-mediated antiviral state may be primarily conferred by autocrine/paracrine signaling mediated by TRIF-dependent synthesis of type I IFN. We therefore examined the ability of AV-C to trigger secretion of type I IFN from exposed cells. For this, we first utilized a cellular LUC-based bioassay to measure subtype-independent bioactive IFN in media harvested from AV-C-treated cells. Figure 6B shows that the compound was able to induce IFN secretion from wild-type fibroblast cells as well as those lacking IPS-1/MAVS or STING but not TRIF, in

agreement with our results described above. In addition, AV-C was also capable of inducing secretion of IFN- β from human peripheral blood mononuclear cells (PBMCs) (Fig. 6C), indicating that this effect is likely cell type independent. Based on these results, we conclude that the antiviral cellular state elicited by AV-C requires TRIF-dependent secretion of type I IFN and subsequent IFNAR-mediated expression of antiviral effectors.

An unexpected finding from these experiments was that the replication of DENV in cells lacking IPS-1/MAVS or IFNAR was >1.5 logs higher than in parental wild-type cells or those lacking STING or TRIF (Fig. 6A). This suggests that the comparatively low replication of the virus in fibroblasts may be due to infection-induced, TRIF- and STING-independent but IPS-1/MAVS and IFN-dependent activity in this cell type (see below). ZIKV also exhibited enhanced growth in cells lacking IPS-1/MAVS and IFNAR, potentially indicating that this represents a flavivirus-specific trait. Importantly, these observations also establish IPS-1/MAVS-deficient cells as a permissive and useful model for assessing the role of TRIF or STING activation in DENV growth, including AV-C-mediated effects. Unfortunately, AV-C did not stimulate observable antiviral effects against CHIKV in C57BL/6J mice, as we have previously shown for the characterized IRF3 agonist DMXAA (5,6-dimethylxanthenone-4-acetic acid) (41) (Fig. S5). Given the requirement for functional IFN signaling, this was likely due to the fact that AV-C was unable to trigger IFN-stimulated gene transcription in murine cells *in vitro* or secretion of serum-associated type I IFN in mice, as also seen with DMXAA (Fig. S4).

FIG S5

In vivo activity of AV-C. (A) Transcription of IFN-inducible genes IP10, IFIT1, and ISG15 in murine RAW 264.7 macrophage-like cells treated for 8 h with universal type I IFN (α IFN) or 25 μ M AV-C. Values displayed are average fold changes versus results in DMSO-treated cells from two biological replicates. (B) Transcription of IP10, IFIT1, and ISG15 in murine RAW 264.7 macrophage-like cells treated for 8 h with serum harvested 6 h posttreatment from C57BL/6J mice injected intraperitoneally with DMXAA or AV-C (25 mg/kg). Values displayed are average fold changes versus DMSO-treated cells of two biological replicates. (C) Average (\pm standard deviations) CHIKV titers from homogenates of the indicated tissues at 3 days postinfection from C57BL/6J mice ($n = 4$) treated intraperitoneally with DMSO or AV-C at 25 mg/kg. Download [FIG S5](#), [PDF file](#), 0.1 MB.

Copyright © 2017 Pryke et al.

This content is distributed under the terms of the [Creative Commons Attribution 4.0 International license](#).

AV-C elicits innate immune reactivity in human peripheral blood mononuclear cells. The ability of innate activating stimuli to induce secretion of immunomodulatory cytokines is strongly predictive of their capacity to initiate and facilitate adaptive immune responses (e.g., adjuvanticity). This is exemplified by the TLR4/TRIF agonist monophosphoryl lipid A (MPL), which is used clinically as a vaccine adjuvant (67). To investigate whether AV-C is capable of similarly inducing innate activation of primary cells relevant to the establishment of adaptive responses, we examined reactivity in human PBMCs. Observation of such activity would represent an important proof of concept for the potential expansion of AV-C's therapeutic utility. As shown in Fig. 7A, AV-C stimulated IRF3 S386 phosphorylation in these cells. Furthermore, Fig. 7B illustrates that AV-C was able to induce transcription of endogenous ISGs in PBMCs (as observed in human fibroblasts) as well as proinflammatory genes IL-6 and IL-1 β . Next, we examined the ability of AV-C to stimulate (i) the secretion of cytokines associated with potentiating adaptive immune responses to microbial pathogens following antigen exposure, as well as (ii) expression of cellular markers indicative of dendritic cell (DC) maturation. This was done using PBMCs from five separate human donors, to control for potentially complicating impacts of biological characteristics known to influence innate immune induction, such as genetic background or age. As shown in Fig. 7C, treatment of these cells for 24 h with AV-C was found to significantly induce secretion of the proinflammatory cytokines tumor necrosis factor alpha (TNF- α), IL-6, and IL-1 β relative to levels in untreated cells from matched donors. Similarly trending results were observed for the TLR4/TRIF stimulus LPS. Interestingly, however, while LPS significantly induced secretion of the anti-inflammatory cytokine IL-10, the same was not true for AV-C. Furthermore, AV-C was also unable to upregulate expression of the maturation markers HLA-DR, CD86, CD80, or CD40 on immature DCs (Fig. S7). These observations suggest that both

TRIF activators LPS and AV-C may fundamentally induce distinct cellular target pathways. Nevertheless, AV-C is capable of stimulating an IRF3-associated innate immune response in primary PBMCs from multiple human donors, thereby magnifying its potential as an immunotherapeutic compound.

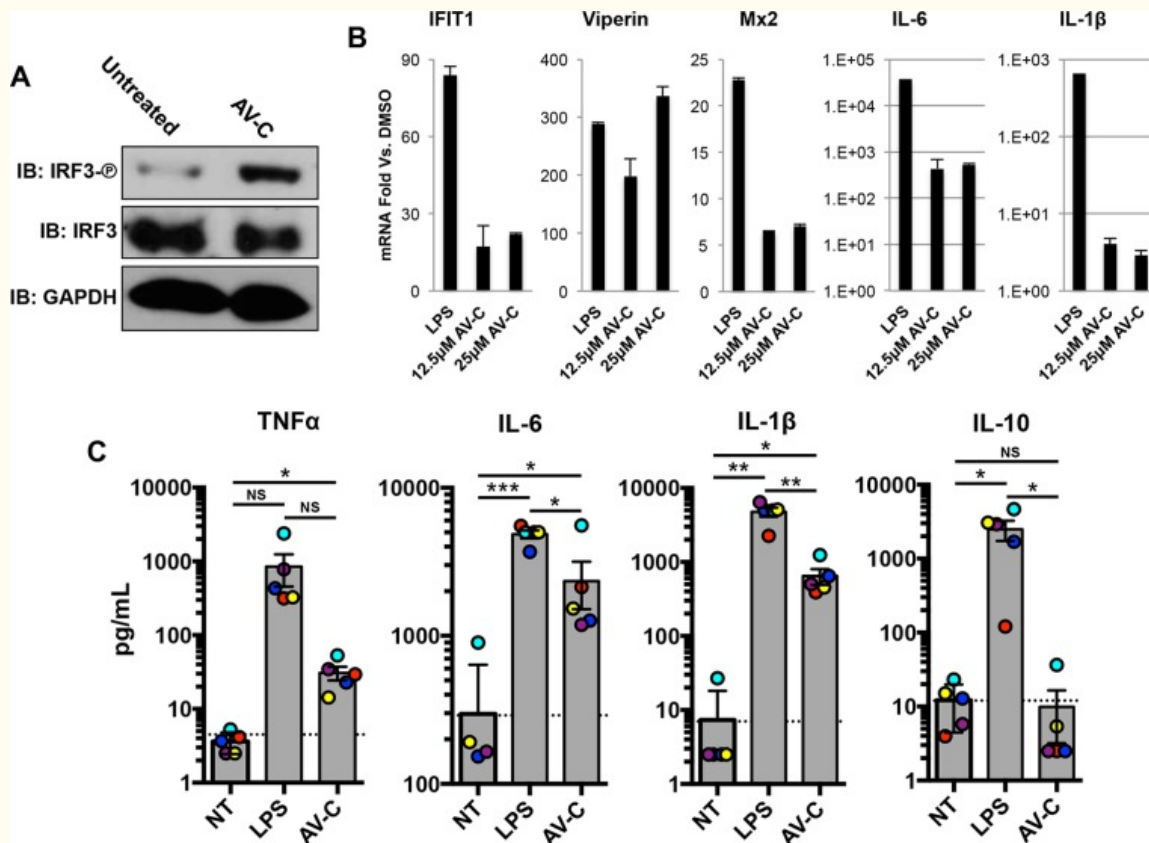


FIG 7

AV-C-mediated innate activation of primary human peripheral blood mononuclear cells. (A) Immunoblot showing the S386 phosphorylation status of IRF3, total IRF3, and GAPDH from human PBMC lysates following 4-h treatment with 1% DMSO or 12.5 μM AV-C. (B) Transcription of IFIT1, viperin, Mx2, IL-6, and IL-1β in PBMCs treated for 8 h with 1 μg/ml LPS, 12.5 μM AV-C, or 25 μM AV-C. Values displayed are average fold changes versus results in DMSO-treated cells of two biological replicates, ± standard deviations. (C) Secretion of TNF-α, IL-6, and IL-1β from PBMCs either left untreated (NT) or exposed for 24 h to 100 ng/ml LPS or 25 μM AV-C. Values presented are averages (in picograms per milliliter) ± the standard deviation from cells from five individual donors (donor-specific values are color coded). Paired-sample Student's *t* test comparisons were made between treated and NT cells. *, $P < 0.05$; **, $P < 0.01$; ***, $P < 0.001$.

AV-C does not trigger canonical activation of NF-κB. NF-κB is a transcription factor that is activated in response to signaling from multiple PRRs, many that also lead to IRF3, and is important for the expression of numerous proinflammatory cytokines (68), including type I IFNs (69). We therefore examined whether exposure of cells to AV-C led to responses indicative of NF-κB activation. As shown in Fig. 8A, THF cells stably transfected with NF-κB-dependent LUC (41) did not respond to AV-C at concentrations above those found to induce IFN-dependent signaling. We next used indirect immunofluorescence to examine the subcellular localization of NF-κB subunit P65 in THFs following AV-C treatment. Figure 8B illustrates that exposure to the established NF-κB-inducing stimulus SeV led to nuclear accumulation of P65, a requisite step in the protein's transcriptional activity. However, nuclear accumulation of the protein was not detected in DMSO- or AV-C-exposed cells, consistent with NF-κB not being activated by these treatments. Intriguingly, NF-κB has been shown to play a role in transcription of cytokines, such as TNF-α, IL-6, and IL-1β, that we found to be secreted

by PBMCs in response to AV-C (Fig. 7C). As such, we decided to ask whether the lack of AV-C-mediated NF- κ B activation was a phenomenon specific to fibroblasts. To address this, we exposed PBMCs from two donors to AV-C at 25 μ M, a concentration that elicited cytokine expression and secretion in these cells (Fig. 7). Control cells were treated with DMSO (negative) or LPS (positive). Whole-cell lysates were then harvested at 20 min, 40 min, and 60 min posttreatment, and immunoblotting was used to examine levels of I κ B α , a factor that sequesters NF- κ B in the cytoplasm and whose ubiquitin-mediated degradation is required for NF- κ B nuclear accumulation. As shown in Fig. 8C, treatment of PBMCs with LPS led to substantial degradation of I κ B α in both donor cells by 60 min. However, treatment with DMSO or AV-C failed to trigger degradation of the protein. Based on these observations, we concluded that AV-C does not induce cellular signaling responses that lead to activation of NF- κ B in either fibroblasts or PBMCs.

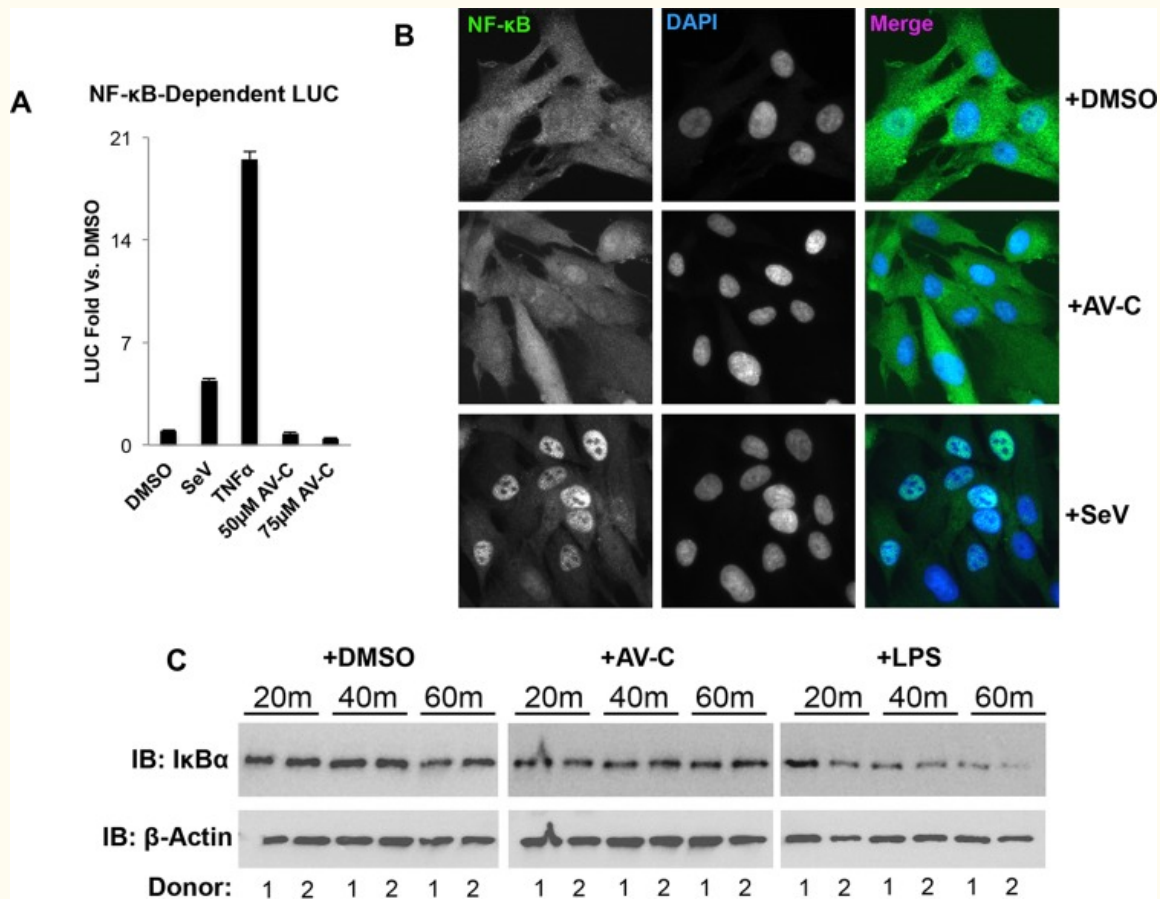


FIG. 8

NF- κ B activity is not induced by exposure to AV-C. (A) Reporter assay results, showing induction of NF- κ B-dependent LUC expression in THF-NF- κ B cells at 8 h posttreatment with 160 HAU/ml SeV, 10 ng/ml TNF- α , or the indicated concentration of AV-C. Values displayed are average fold changes (\pm standard deviations) based on three replicates compared to DMSO-treated cells. (B) Subcellular localization of NF- κ B subunit P65 in THF cells following 4-h exposure to 1% DMSO, 160 HAU/ml SeV, or 25 μ M AV-C. (C) Degradation of I κ B α in PBMCs from two donors following exposure to 1% DMSO, 12.5 μ M AV-C, or 100 ng/ml LPS for the indicated time (β -actin served as the loading control).

DISCUSSION

The ongoing transmission of multiple arboviruses in Latin America and the Caribbean underscores the value of developing therapeutic strategies that display broad-spectrum efficacy. Unfortunately, the fact that the current outbreak involves unrelated virus families (i.e., *Togaviridae*, *Flaviviridae*) that exhibit unique replication

characteristics has made identification of multitarget, directly acting antiviral molecules more problematic. Fortunately, the type I IFN system, as part of the overall innate immune response, evolved to effectively block replication by diverse viral pathogens, including flaviviruses and alphaviruses (70, 71). Clinical utilization of IFN itself is, however, associated with significant undesirable attributes, including high cost, dosing feasibility, and adverse side effects (30, 31, 72). Nevertheless, the potency of IFN-induced processes renders them druggable yet underutilized therapeutic targets (33). Furthermore, the high probability of sensitivity of unknown yet potentially emerging viral pathogens (or bioweapons) to the IFN-induced cellular state provides another motivation for drug discovery endeavors with this focus. The ability of innate immune stimuli to yield other immunotherapeutic outcomes, such as adjuvanticity and antitumor activity, adds still further incentive to their discovery and characterization (73). Our group and others have pursued novel agonists of IRF3-terminal pathways as treatments against RNA viruses, including DENV (35, 38, 74) and CHIKV (36, 37, 41). However, the current study represents the first application of this approach to ZIKV. Moreover, while molecules described thus far as efficacious are agonists of the IPS-1/MAVS or STING pathways, our study describes a novel synthetic compound that induces TRIF-dependent responses. Indeed, TRIF may represent a curiously underemphasized cellular target for combating DENV, ZIKV, and alphavirus infections. This is due to the fact that while virus-inhibitory phenotypes have been described that are directed at IPS-1/MAVS (75, 76) and STING (77), TRIF-targeting mechanisms have thus far not been identified in these viruses to our knowledge. This is supported by our observation that replication of DENV and ZIKV appears similar in wild-type cells and those lacking TRIF (Fig. 6). As such, TRIF-dependent activation of the IFN response could be a more potent antiviral strategy, since this pathway may be less vulnerable or even invulnerable to disruption by these viruses.

Initially, our work retrieved multiple small molecules capable of inducing IFN-dependent reporter signaling (see Fig. S1 in the supplemental material), and many of these are being actively characterized in our laboratory. AV-C was found to robustly generate consistent responses in multiple cell types, and we therefore concentrated our efforts on understanding its mode of action and therapeutic potential. We began by examining the cellular transcriptional response induced by the molecule and the similarities shared with that induced by type I IFN. While a larger set of genes regulated by IFN treatment was uncovered, a substantial subset was found to be co-upregulated by AV-C treatment, including many that confer direct antiviral activity, as well as IFN- β itself (Fig. 2B). Importantly, some of these (including IFN- β) were reflected in corresponding AV-C-induced protein translation (Fig. 2C and 6C), suggesting that despite upregulation of a limited group of IFN-stimulated genes, AV-C may generate a cellular environment antagonistic to virus growth. We therefore examined replication of CHIKV, DENV, and ZIKV on fibroblasts pretreated with AV-C to determine whether this effect was evident. As shown in Fig. 3, all three viruses grew to diminished levels in AV-C-pretreated THF cells, with CHIKV displaying the highest sensitivity to the compound. Interestingly, the overall impairment of ZIKV growth was less pronounced than that observed for CHIKV. This observation may be consistent with the encoding of phenotypes by ZIKV (such as a block to STAT2 function [78]) that enhance its resistance to IFN-induced cellular states. The extent to which viral mechanisms are involved in the resistance of ZIKV to IFN-stimulated cells will require a more focused deconstruction.

Activation of IFN and IFN-dependent genes can occur by way of multiple transcription factors and signaling pathways. To elucidate the cellular proteins involved in the AV-C-associated antiviral state under the hypothesis that IFN is involved, we examined specific components of the best-characterized IFN-terminal signaling cascades. IRFs, including IRF1, IRF5, IRF7, and IRF3, as well as NF- κ B, have been implicated in the transcriptional induction of IFN genes (reviewed in reference 68). We first examined the activation status of IRF3 and found that, as with conventional stimuli of the STING, IPS-1/MAVS, and TRIF pathways, AV-C did in fact induce phosphorylation of the protein in fibroblasts (Fig. 4A). Whether IRF3 and its activation by AV-C are actually required for transcriptional induction were separate questions that we addressed by using cells that lacked the IRF3 protein as well as using a chemical inhibitor of TBK1/IKK ϵ (BX795). In both of these experiments, AV-C failed to activate expression of an IFN-dependent reporter or endogenous mRNAs. Furthermore, AV-C-associated IRF3 phosphorylation was also abrogated in the presence of BX795 (Fig. 4). Collectively these results indicate that AV-C triggers an IRF3-terminal pathway, of which three primary PRR- and adaptor-associated ones are known. We therefore next focused on addressing whether any of these was necessary for the AV-C-induced innate activation phenotype.

An understanding of the target cellular pathway activated by AV-C represents critical information that allows wider predictions to be made about tissue states and phenotypes elicited by the molecule. For example, dsRNA can lead to disparate outcomes, including transcription-independent effects, such as apoptosis and Src-mediated cell migration, depending on whether it activates the RIG-I/IPS-1/MAVS- or TLR3/TRIF-dependent pathways (79). *In vivo*, the RIG-I and TLR3 ligands can also produce distinct adaptive immune response profiles to coadministered vaccine antigens (80, 81). Furthermore, secretion of dissimilar cytokine profiles is evident following STING-mediated versus TLR/TRIF-mediated stimulation (40, 82). In light of these findings, we aimed to identify the adaptor-associated signaling pathway(s) required for AV-C-induced IRF3 activation. We found that AV-C-induced transcription and IRF3 phosphorylation were operational in cells lacking either STING or IPS-1/MAVS (Fig. 5). In the absence of TRIF, however, innate stimulation by AV-C as defined by these activities was eliminated. Whether AV-C also triggers related adaptors, such as MyD88, or upstream PRRs, such as TLR3 or TLR4, is currently being examined. Recent work has uncovered a functional role for TRIF in STING-dependent innate activation (83). Our data reveal no obvious differences in AV-C-mediated innate induction or biological activity between wild-type cells and those lacking STING (Fig. 5 and 6), suggesting that the compound activates a TRIF-specific pathway independently of STING.

AV-C treatment leads to TRIF-dependent transcription of IFN- β (Fig. 2) as well as antiviral ISGs that are known to inhibit flavivirus and alphavirus replication (84,–86). We therefore asked whether the TRIF, IPS-1/MAVS, and STING signaling pathways are necessary for the AV-C-associated antiviral phenotypes we observed (Fig. 3). As shown in Fig. 6, cell lines lacking each individual protein were able to establish canonical IFN-induced antiviral states as indicated by the strong inhibition of all three viruses following pretreatment with IFN- β , indicating that JAK/STAT signaling is functional. AV-C was also able to induce equivalent (and perhaps more potent) antiviral activity in cells lacking IPS-1/MAVS and STING, indicating that these proteins are dispensable for antiviral effects conferred by AV-C, in agreement with results presented in Fig. 5. Interestingly, AV-C induced the expression of antiviral genes, such as viperin, IFIT1, and ISG15, that can be transcribed in an IRF3-dependent, IFN-independent manner (65, 66). Moreover, growth of all three viruses was highly susceptible to cellular states elicited by IFN- β pretreatment (Fig. 6A). We therefore examined whether IFN-induced (JAK/STAT-mediated) signaling was, along with TRIF signaling, a mechanistic requirement for the antiviral state associated with AV-C exposure. To address this, we constructed cells from which the IFNAR protein was deleted and were correspondingly unable to react to type I IFN, as demonstrated by the failure to establish an IFN-induced antiviral state. As shown in Fig. 6A, the antiviral effect of AV-C was also abrogated in these cells, suggesting that AV-C-induced, TRIF/IRF3-dependent secretion of type I IFN is responsible for the compound's activity. To further validate this conclusion, we examined whether cells exposed to AV-C actually secreted bioactive type I IFN in detectable quantities. We first utilized a cell-based bioassay to show that AV-C-treated wild-type THF cells as well as those lacking IPS-1/MAVS or STING, but not TRIF, secreted type I IFN (Fig. 6B). Additionally, human PBMCs exposed to AV-C secreted IFN- β , demonstrating that multiple cell types respond in this way (Fig. 6C). Collectively, these results are consistent with a model of AV-C-mediated activity that involves TRIF-dependent but STING- and IPS-1/MAVS-independent synthesis and secretion of type I IFNs that generate an antiviral cellular state through ISG expression following engagement of the IFNAR and ensuing JAK/STAT signaling.

Unfortunately, wild-type fibroblasts represent a less useful substrate for growth of DENV. Our experiments revealed, intriguingly, that this is likely due to the virus' inability to counteract infection-induced, IFN-mediated antiviral responses in these cells. DENV growth was enhanced by nearly 2 logs in THFs engineered to lack either IPS-1/MAVS or IFNAR (Fig. 6A) (87, 88). These results align well with the observation that DENV is extremely sensitive to the IFN-induced state in fibroblasts (Fig. 6A), as well as previous reported findings showing that the IPS-1/MAVS/IRF3 signaling axis is crucial to flavivirus-associated IFN induction (76, 89, 90). Importantly, this also indicates that THF-ISRE- Δ IPS1 cells represent a sound model for examining the antiviral effect of AV-C since (i) they are capable of responding to AV-C-induced, IRF3-terminal signaling (Fig. 5), (ii) their IFN-induced signaling is intact, and (iii) they support high-titer DENV growth. Enhanced replication of ZIKV, a related flavivirus, was also observed in the absence of either IPS-1/MAVS or IFNAR, indicating that it may, as expected, trigger IPS-1/MAVS-dependent IFN synthesis. Replication of CHIKV did not differ significantly between the mutant cell lines, despite the fact that the virus is highly sensitive to the IFN-induced phenotype (Fig. 6A). This may have been due to the nonspecific nature of the virus' innate evasion strategy, which involves rapid and indiscriminate shutdown of cellular gene transcription and translation (56). Whether CHIKV exhibits IRF3-terminal pathway-targeted inhibition has not been demonstrated to our knowledge.

TRIF-inducing stimuli may possess immunotherapeutic potential beyond direct antiviral activity (91,–93). For instance, the TLR3/TRIF agonist poly(I-C) shows beneficial effects in mouse models of arthritis (94), colitis (95), bacterial infection (96), and wound healing (97, 98). Likely more impactful are the potentiating effects of TRIF stimulation on establishment of adaptive immunity to infectious agents, as illustrated by the TLR4/TRIF agonist MPLA, an FDA-approved component of vaccines against papillomavirus (99) and hepatitis B virus (67). The fundamental mechanistic basis for the adjuvant activity conferred by MPLA is TRIF- and MyD88-mediated synthesis of proinflammatory cytokines and chemokines that drive recruitment and maturation of myeloid-derived antigen-presenting cells (100,–102). Ultimately, this leads to an enhancement of antigen-associated T cell activation, clonal expansion, and Th1 polarization (67, 103). To investigate whether AV-C can induce cellular responses predictive of these immune effects, we examined both secretion of relevant cytokines from primary PBMCs collected from human patients as well as expression of cellular markers that signify DC maturation. As illustrated in Fig. 7, AV-C induced both IRF3 phosphorylation in PBMCs as well as transcription of IFN-stimulated genes IFIT1, viperin, and Mx2. The compound also triggered secretion of key proinflammatory molecules TNF- α , IL-6, and IL-1 β (Fig. 7C), suggesting that it may elicit responses contributory to increased antigen immunogenicity. Interestingly, the innate reactivity to AV-C diverged qualitatively from that induced by the TLR4/TRIF agonist LPS. Transcription of IL-6 and IL-1 β was strongly activated by LPS, but much less so by AV-C (Fig. 8B), and while LPS led to secretion of IL-10, AV-C did not (Fig. 8C). Furthermore, AV-C also failed to stimulate expression of DC maturation markers HLA-DR, CD86, CD80, and CD40 on immature DCs and did not elicit secretion of IL-12p70 from these cells (Fig. S6). These differences underscore the need for more thorough characterization of the molecule in the context of adaptive immune processes to more completely evaluate its potential as an immunotherapeutic agent.

FIG S6

AV-C does not induce maturation of myeloid dendritic cells or secretion of IL-12p70. (A) Myeloid dendritic cells differentiated from healthy human PBMCs were treated with 1% DMSO or stimulated with 0.5 μ g/ml LPS plus 40 ng/ml IFN- γ and 12.5 μ M or 25 μ M AV-C for 20 h. DCs were harvested and analyzed by flow cytometry for the upregulation of surface HLA-DR as well as the costimulatory molecules CD86, CD80, and CD40. Values presented are average mean fluorescence intensities (MFI) \pm the standard deviations for the indicated marker from five individual donors (donor-specific values are represented by clear circles). (B) Myeloid dendritic cells differentiated from healthy human PBMCs were treated as described for cells shown in panel A for 20 h. Culture supernatants were analyzed for the level of IL-12p70 via an ELISA. Values presented are average picograms per milliliter \pm the standard deviation from cells of four individual donors (donor-specific values are represented by clear circles). Paired-sample Student's *t* test comparisons were made between DMSO-treated and stimulated cells. ns, nonsignificant; *, $P < 0.05$; **, $P < 0.01$; ***, $P < 0.001$. Download [FIG S6, PDF file, 0.7 MB](#).

[Copyright](#) © 2017 Pryke et al.

This content is distributed under the terms of the [Creative Commons Attribution 4.0 International license](#).

The induction of proinflammatory cytokines such as TNF- α , IL-6, and IL-1 β by AV-C suggests the involvement of signaling pathways or transcription factors beyond IRF3 alone. Unexpectedly, AV-C failed to induce outcomes such as secretion of IL-10 and IL-12p70 that were induced by TLR4/TRIF agonist LPS (Fig. 7; Fig. S6). These results may represent differential impacts of MyD88 in associated signaling induced by the two stimuli, since secretion of some proinflammatory cytokines, such as IL-10, is known to be abrogated in cells lacking MyD88 (104,–106). Based on the reported role of NF- κ B in transcription of proinflammatory genes such as TNF- α , IL-6, IFN- β , and IL-1 β , which are induced by AV-C as well, as well as dependence on TRIF and MyD88 signaling, we decided to examine whether the compound led to activation of this factor. Surprisingly, we were unable to detect indicators of AV-C-induced NF- κ B activation in either THFs or PBMCs (Fig. 8). These results may be suggestive of the absence of involvement of MyD88 in the AV-C-stimulated response, since NF- κ B induction represents a process enhanced by MyD88 rather than TRIF activity (60, 107). This is also consistent with the differential induction of IL-10 by AV-C and LPS, the expression of which has been linked to NF- κ B activity in immune and other cells (108,–110). With regard to the co-upregulation of TNF- α , IL-6, and IL-1 β by AV-C and LPS, NF- κ B-

independent roles for other transcription factors, such as IRF1 and IRF5, in the expression of such proinflammatory cytokines have been described ([111](#), [112](#)). Whether AV-C is capable of activating other IRFs such as these is certainly possible but requires specific examination.

An a